applied sciences

MDPI

Article

Analysis of the Dynamic Stiffness, Hysteresis Resonances and Complex Responses for Nonlinear Spring Systems in Power-Form Order

Qingtao Wang [1,2], Zhiyong Zhang [1,2,*], Yongheng Ying [1,3] and Zhaojun Pang [2,4]

[1] School of Science, Nanjing University of Science and Technology, Nanjing 210094, China; qtwang@njust.edu.cn (Q.W.); yingyongheng@126.com (Y.Y.)
[2] Institute of Launch Dynamics, Nanjing University of Science and Technology, Nanjing 210094, China; pangzj@njust.edu.cn
[3] Zhejiang Sany Equipment Co., Ltd., Huzhou 200120, China
[4] School of Mechanical Engineering, Nanjing University of Science and Technology, Nanjing 210094, China
* Correspondence: zhiyzhang@njust.edu.cn

Abstract: Power-form nonlinear contact force models are widely adopted in relatively moving parts of macro (e.g., rolling bearings considering Hertzian contact restoring force between rolling elements and bearing raceways) or micro (e.g., the micro cantilever probe system of atomic force microscopy) scale mechanical systems, and contact resonance could cause serious problems of wear, contact fatigue, vibration, and noise, which has attracted widespread attention. In the present paper, the softening/hardening stiffness characteristics of continuous and one-sided contact power-form nonlinear spring models are addressed, respectively, by the analysis of the monotone features of resonant frequency-response skeleton lines. Herein, the period-n solution branch and its stability characteristics are obtained by the harmonic balance and alternating frequency/time domain (HB–AFT) method and Floquet theory. Compared with previous studies, this paper will furtherly clarify the influences of externally normal load, the power form exponent term, and excitation amplitude on the softening/hardening stiffness characteristics of general power-form spring systems. In addition, for a power-form system with a one-sided contact, the phenomena of primary and super/sub-harmonic hysteretic resonances inducing period-doubling, folding bifurcation, the coexistence of multiple solutions are demonstrated. Besides, it gives the evolution mechanism of two types of intermittency chaos in a one-sided contact system. The overall results may have certain basic theoretical significance and engineering values for the control of vibration and noise in contact mechanical systems.

Keywords: power-form nonlinear spring; dynamic stiffness; hysteretic resonance; one-sided contact; intermittency chaos

check for updates

Citation: Wang, Q.; Zhang, Z.; Ying, Y.; Pang, Z. Analysis of the Dynamic Stiffness, Hysteresis Resonances and Complex Responses for Nonlinear Spring Systems in Power-Form Order. *Appl. Sci.* **2021**, *11*, 7722. https://doi.org/10.3390/app11167722

Academic Editors: Roman Starosta and Jan Awrejcewicz

Received: 25 July 2021
Accepted: 20 August 2021
Published: 22 August 2021

Publisher's Note: MDPI stays neutral with regard to jurisdictional claims in published maps and institutional affiliations.

Copyright: © 2021 by the authors. Licensee MDPI, Basel, Switzerland. This article is an open access article distributed under the terms and conditions of the Creative Commons Attribution (CC BY) license (https://creativecommons.org/licenses/by/4.0/).

1. Introduction

The mass-spring model is one of the basic mechanical elements, which can be used to describe the interaction of deformation, energy transfer, and motion control between different bodies. At the macro, micro, and nano scales, linear spring models with a linear relationship between force and displacement depicted by hook's law $F(x) = kx$ are widely observed [1]. However, many interactions are not suitable for linearization. The classical three-body problem mentioned by Newton in 1687 promotes the development of nonlinear science [2]. The nonlinear load-deformation relationship is generally expressed as $F(x) = a_n \cdot x^n + a_{n-1} \cdot x^{n-1} + \ldots + a_2 \cdot x^2 + a_1 \cdot x + a_0$. In a contact system, however, the power-form nonlinear restoring force $F_C(x) = K_C \cdot x^\alpha$ is more common, where the nonlinear power-form exponent term α of the normal contact force between two elastic surfaces is in the range of 1.5 to 3.5 [3], the nonlinear force in piano hammers is $2.2 < \alpha < 3.5$ [4], and even the case of $2 < \alpha < \infty$ exists in the solitary wave propagation through particle chains [5].

Contact interfaces are indispensable in machine systems including bolted joints, hinges, rolling bearings, and so on, which can transmit coupling forces between structures [6]. Many publications have focused on the contact stiffness modelings and their static or quasi-static stiffness characteristics for contact systems [7,8]. On the other hand, it should be noted that in the fundamental mechanisms with relative motions (e.g., hinges, meshing gears, rolling bearings, and probe detection system), the contact vibrations between relative moving components are often inevitable, due to the external excitation or roughness and waviness between contact surfaces [9]. Herein, the dynamic contact dynamic stiffness has a significant effect on the dynamic behavior of the contact machine system, and the static stiffness model is unable to describe the dynamic characteristics in contact vibrations. For example, it is traditionally considered that the rolling bearings have hardening stiffness characteristics due to the Hertzian contact force–deformation relationship [7,10], but gradually researchers find that the dynamic supporting characteristics of the system can soften [11,12]. In addition, recently contact resonances have been widely used in the design of sensors [13] and atomic force microscopy [14], and obviously, contact dynamic stiffness is closely correlative to the contact resonance, but this correlation needs to be further clarified. Therefore, it is necessary to conduct a systematic study on the nonlinear dynamic stiffness and resonance behaviors of a nonlinear power-form mass-spring system especially considering contact factors.

Based on the works of Mickens [15] and Hu et al. [16], Cveticanin [17] and Kovacic et al. [18] gave the approximate analytical solution of the general power-form continuous system with the aid of special function method. Then, Kovacic [19], Rakaric et al. [20] and Huang et al. [21] carried out many studies on the hysteretic characteristics of the primary resonances for such a general power-form system. However, the above research has not considered the effect of externally normal load on the dynamic stiffness and resonances. On the other hand, most of the studies of contact vibrations are concentrated on the Hertzian point contact case with the ideal 3/2 power-form exponent term. Carson and Johnson [22] proposed the concepts of contact spring and contact resonance earlier, considering the rolling contact between two disks. Through experiment, it is found that this Hertzian point contact system has dynamic softening stiffness in small contact resonance, whose characteristics are very different from the static hardening stiffness. It is also pointed out that the case of loss contact can increase the softening spring characteristics. Soon afterward, Nayak [23] verified the results of Carson and Johnson [22] by the analysis of a nonlinear one-sided Hertzian point contact spring model under harmonic excitations, in which the author provided an analytical study on the softening hysteresis characteristics of the system in primary resonances. For Nayak's contact spring model, Hess and Soom [9] found that the dynamic load components can lead to a reduction in the mean area of contact and the friction force. Rigaud and Perret-Liaudet [24] pointed out that loss of contact non-linearity can bring a wide frequency range of softening resonance. Furtherly, Ma [25] discussed the criterion for contact loss to occur. In a word, the Hertzian point contact system has softening contact resonance characteristics in the case of small vibration, and the normal constant load has a significant influence on the dynamic stiffness of the system, but the influence law needs to be further developed. In addition, there are few studies on the characteristics of contact resonances for a general power-form contact spring system.

The contact resonance and its hysteresis behaviors can aggravate the wear, contact fatigue, vibration, and noise of a mechanical system, and as a consequence, affect the working accuracy of the system. Therefore, it is of great theoretical and engineering value to study contact resonance in depth. In this paper, the harmonic balance and alternating frequency/time domain (HB–AFT) method [25,26] and Floquet theory are used to further study the primary, super-harmonic and sub-harmonic resonances and their dynamic stiffness (i.e., the resonant skeleton) characteristics in continuous and one-sided contact power-form nonlinear spring models. For doing these, firstly, the influence of the normal constant load on the dynamic softening/hardening stiffness characteristics will be discussed. Secondly, the inherent mechanism of hysteretic resonances will be studied. Finally,

the evolution of complex responses even the intermittency chaos in a one-sided contact system will be clarified.

2. Power-Form Nonlinear System Model

For a power-form nonlinear spring-mass system with an externally normal load W and a harmonic excitation, its equation of motion is given as

$$\frac{d^2x}{dt^2} + 2\zeta H(x)\frac{dx}{dt} + H(x)\mathrm{sgn}(x)|x|^{\alpha} = A\cos\omega t + W \tag{1}$$

where ζ is the damping coefficient; A and ω are the amplitude and frequency of harmonic excitation, respectively; sgn(x) is the sign function as,

$$\mathrm{sgn}(x) = \begin{cases} 1, & x > 0 \\ 0, & x = 0 \\ -1, & x < 0 \end{cases}. \tag{2}$$

$H(x) \in \{1, \mathrm{Heaviside}(x)\}$, herein $H(x)$ takes 1 for the continuous system, and if $W = 0$, the Equation (1) is consistent with the classical model of reference [19]. For a one-sided contact system, $H(x)$ takes as a Heaviside function of x,

$$\mathrm{Heaviside}(x) = \begin{cases} 1, & x > 0 \\ 0, & x \le 0 \end{cases} \tag{3}$$

and in this case, the system loses contact when $x < 0$ (see Figure 1).

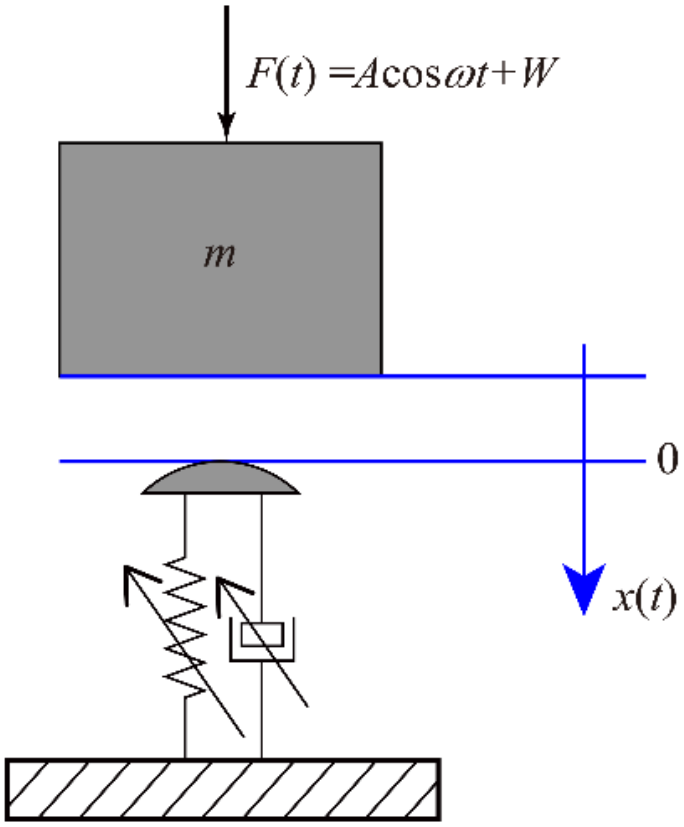

Figure 1. Power-form nonlinear one-sided contact system.

3. Methodology

The AFT technique can avoid the analytical treatment of nonlinear terms through time-domain discretization [26], and this makes the HB-AFT method very effective in solving the strong nonlinear contact problem, which is different from the traditional harmonic balance method. In this paper, the periodic solution is called the period-n solution if the period of the response is n times the excited period. The solution process of the period-1 motion of Equation (1) is given below.

Let $\tau = \omega \cdot t$, then Equation (1) can be expressed as

$$\omega^2 \frac{d^2 x(\tau)}{d\tau^2} + F(x(\tau)) = A\cos\tau + W. \tag{4}$$

where the nonlinear restoring force is

$$F(x(\tau)) = 2\zeta\omega H(x(\tau))\frac{dx(\tau)}{d\tau} + H(x(\tau))\mathrm{sgn}(x(\tau))|x(\tau)|^{\alpha}. \tag{5}$$

To find the periodic solution of Equation (4) with period 2π, $x(\tau)$ and $F(\tau)$ can be expressed as

$$x(\tau) = \boldsymbol{P}(1) + \sum_{k=1}^{K} [\boldsymbol{P}(2k)\cos(k\tau) - \boldsymbol{P}(2k+1)\sin(k\tau)] \tag{6}$$

$$F(\tau) = \boldsymbol{Q}(1) + \sum_{k=1}^{K} [\boldsymbol{Q}(2k)\cos(k\tau) - \boldsymbol{Q}(2k+1)\sin(k\tau)] \tag{7}$$

According to the process of harmonic balance, insert Equations (6) and (7) into Equation (4) and obtain the following $2K + 1$ algebraic relationships:

$$\boldsymbol{g}(\boldsymbol{P}, \boldsymbol{Q}, \omega) = 0 \tag{8}$$

Equation (8) consists of $2K + 1$ algebraic equations but contains $4K + 2$ unknown harmonic coefficients denoted as $\boldsymbol{P}$ and $\boldsymbol{Q}$ in Equations (6) and (7). To obtain $\boldsymbol{P}$ from Equation (8), the following AFT process is adopted.

The time-domain discrete information of $x(\tau)$ is given by the inverse discrete Fourier transform as,

$$x(n) = \mathrm{Real}\left\{ \boldsymbol{P}_0 + \sum_{k=1}^{K} \boldsymbol{P}_k e^{i(2\pi kn/N)} \right\} \tag{9}$$

and the discrete information of the restoring force in time domain is

$$\boldsymbol{F}(n) = \boldsymbol{F}(\boldsymbol{X}(n), \boldsymbol{X}'(n), \omega) \tag{10}$$

Then, by discrete Fourier transform, $\boldsymbol{Q}$ can be expressed as

$$\boldsymbol{Q}_k = \frac{\phi}{N} \sum_{n=0}^{N-1} \boldsymbol{F}(n)\, e^{i(-2\pi kn/N)} \tag{11}$$

Herein, $\phi_k = \phi\,(2k) + i\,\phi\,(2k+1)$; $\phi_0 = \phi\,(1)$, where ϕ takes $\boldsymbol{P}$ or $\boldsymbol{Q}$ in Equations (9) and (11); N is the number of sampling points in a time domain period, and $n = 0, \ldots, N-1$; $\phi = 1$ when $n = 0$, otherwise $\phi = 2$.

Taking $\boldsymbol{P}$ as an unknown variable and ω as a control parameter, the arc-length continuation can be introduced to Equation (8) for automatically tracking $\boldsymbol{P}$ and the frequency-response curve of system (4).

Finally, the stability characteristics of the frequency-response curve can be obtained by Floquet theory [26].

4. Results

4.1. Frequency-Response Characteristics of Continuous System (H(x) = 1, ζ = 0.01, A = 0.1)

For $\alpha = 1.5$ and $W = 0$, the continuous system is power-form nonlinear without externally normal load. Its primary resonance exhibits hardening spring characteristics since the period-1 frequency-response curve bends to the right (see Figure 2a), and cyclic folding bifurcations at turning points A_1 and A_4 can bring jumping phenomena to the system. For $\alpha = 0.6$ and $W = 0$, as shown in Figure 2b, the primary resonance of the system exhibits softening spring characteristics, and the 2-order, 3-order, and 5-order super-harmonic resonances are excited obviously. Herein, transcritical bifurcations at A_5 and A_6 lead period-1 solution unstable and 2-order superharmonic resonance emerging. Overall, as $\alpha > 1$ (or $0 < \alpha < 1$), the resonant skeleton line of the primary resonant frequency-response curve has no inflection point, i.e., the system has a single monotonic softening (or hardening) dynamic stiffness characteristic, respectively, but the hysteretic degree can be adjusted by α. As shown in Figure 3, the resonant curves gradually slope more to the right and the resonant amplitudes decreases as α increases, i.e., the hardening spring characteristics get stronger. The above results agree well with the theoretical studies of the literature [19].

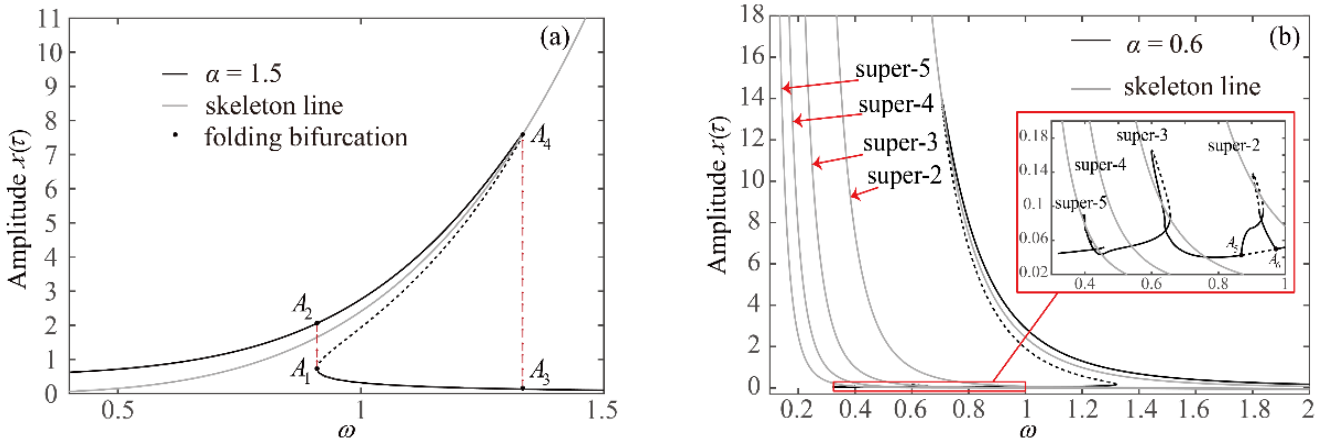

Figure 2. For $W = 0$, stable (solid) and unstable (dashed) periodic frequency-response peak-to-peak curves of continuous system, (**a**) $\alpha = 1.5$ and (**b**) $\alpha = 0.6$.

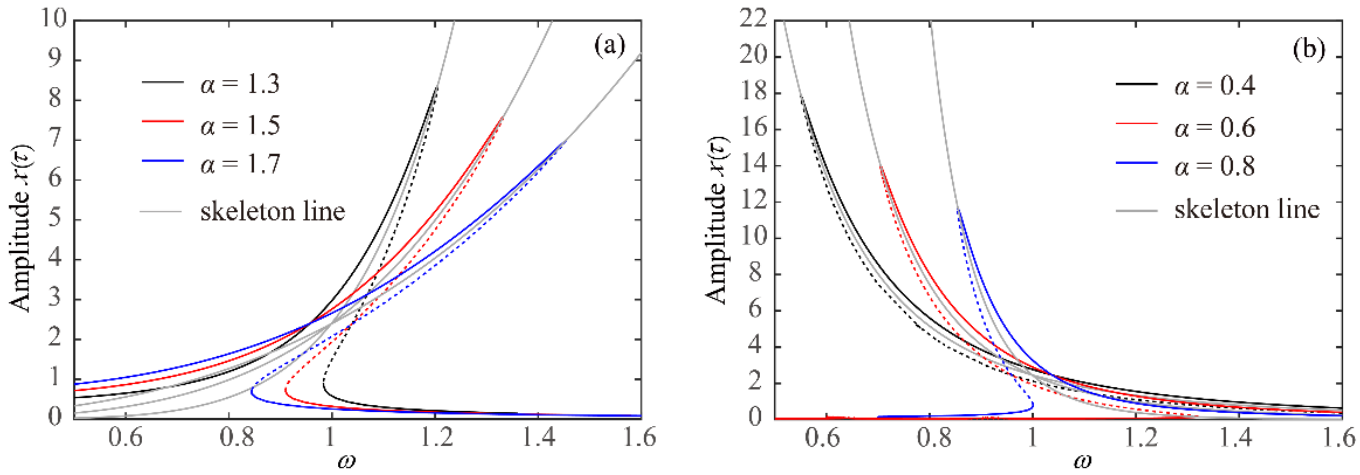

Figure 3. For $W = 0$, influence of α on the frequency-response peak-to-peak curves of continuous system, (**a**) $\alpha > 1$ and (**b**) $0 < \alpha < 1$.

As shown in Figure 4, when a constant load is applied (i.e., $W > 0$), an inflection point appears and the skeleton line of the primary resonant frequency-response curve bends from left to right (for $\alpha > 1$) or right to left (for $0 < \alpha < 1$), which changes the dynamic stiffness characteristics of the continuous system. For example, when $\alpha = 1.5$ and $W = 5$, the response amplitude is lower than the inflection point of the skeleton line, which makes the system have a softening spring (i.e., softening dynamic stiffness) characteristics (see Figure 4a). However, if the response amplitude is higher than the inflection point of the skeleton line (when $\alpha = 1.5$ and $W = 1$), the system has a softening-to-hardening spring (i.e., softening-to-hardening dynamic stiffness) characteristics (see Figure 4a), and in this case, cyclic folding bifurcations occur at four turning points of the resonant frequency-response curve. On the other hand, when $0 < \alpha < 1$, as shown in Figure 4b, the frequency-response skeleton lines of the primary resonances have the hardening-to-softening characteristics, which makes the system have a hardening dynamic stiffness characteristic when the response amplitude is lower than the inflection point of the skeleton line (such as B_3 point when $W = 1$). Besides, for $\alpha > 1$ (or $0 < \alpha < 1$), the locations of the primary resonances move to high frequency (or low frequency) as the externally normal constant load W increases.

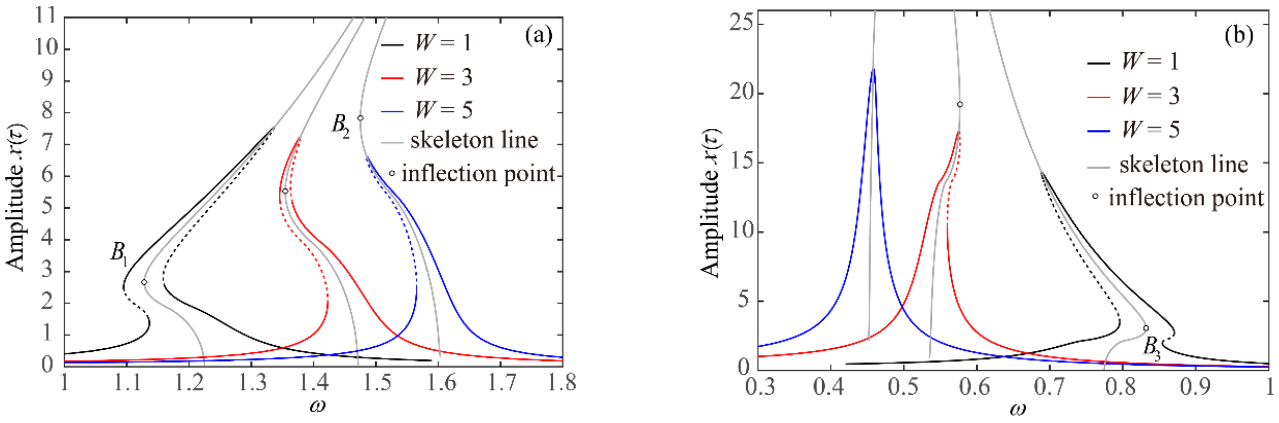

Figure 4. Influence of normal load W on α the frequency-response peak-to-peak curves of continuous system, (**a**) $\alpha = 1.5$ and (**b**) $\alpha = 0.6$.

4.2. Frequency-Response Characteristics of One-Sided Contact System (H(x) = Heaviside(x), ζ = 0.032, A = 0.1, W = 1)

For $\alpha = 1$, the continuous system is linear, so its dynamic stiffness is consistent with the static stiffness of the system. There are no hardening/softening stiffness characteristics, and the skeleton of the primary resonant frequency-response curve is a straight line $\omega = 1$ (see Figure 5a). In contrast, for a power-form $\alpha = 1$ one-sided contact system, an inflection point appears at the boundary of loss contact and the skeleton line of the primary resonant frequency-response curve bends to the left. Therefore, the system exhibits softening dynamic stiffness characteristics in the loss contact case, which is caused by the average contact time decreasing as the vibration amplitude increases [24]. Similarly, for $\alpha > 1$ or $0 < \alpha < 1$, as shown in Figure 5b,c, dramatically softening dynamic stiffness characteristics are exhibited in the loss contact case (compared with the continuous system). Especially, for $\alpha > 1$, the one-sided contact system can have monotonic softening stiffness characteristics (see Figure 5b). This softening dynamic support has been found in the ball bearing-rotor system, where the nonlinearity of Hertzian point contact exists between the balls and raceways of the support ball bearings [27].

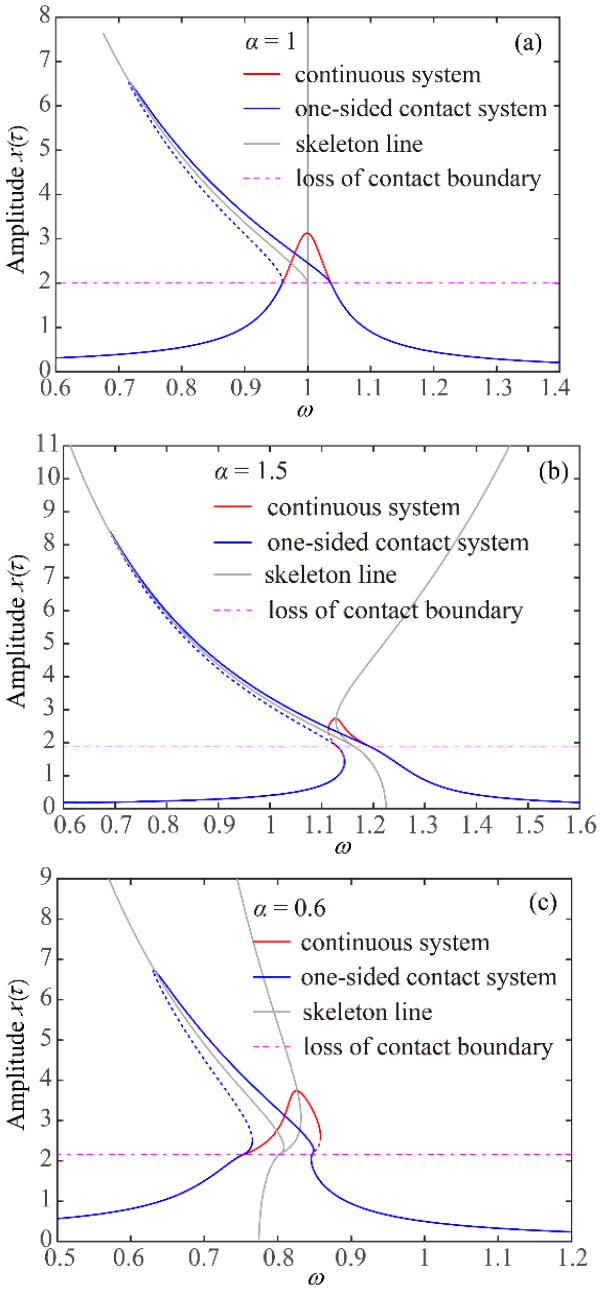

Figure 5. Comparisons of frequency-response peak-to-peak curves between continuous system and one-sided contact system, (**a**) $\alpha = 1$, (**b**) $\alpha = 1.5$, and (**c**) $\alpha = 0.6$, where the magenta dash line denotes the loss contact boundaries.

As shown in Figures 6 and 7, with the increase in the externally normal constant load W, the location of the primary resonance moves to a high frequency ($\alpha > 1$) or low frequency ($0 < \alpha < 1$), which agrees with the rule of the continuous system in Section 4.1. In addition, for the one-sided contact system, it is obvious that the amplitude boundary of loss contact increases as normal load W increases, which means that there is less chance of losing contact. Moreover, the damping coefficient ζ has a significant effect on the response amplitude of a one-sided contact system in the case of loss contact (see Figures 6a and 7a). Therefore, the identification and control of the damping coefficient are very important for the quality control of the practical one-sided contact system with high accuracy requirement, such as the micro-cantilever probe system in the atomic force microscope [28].

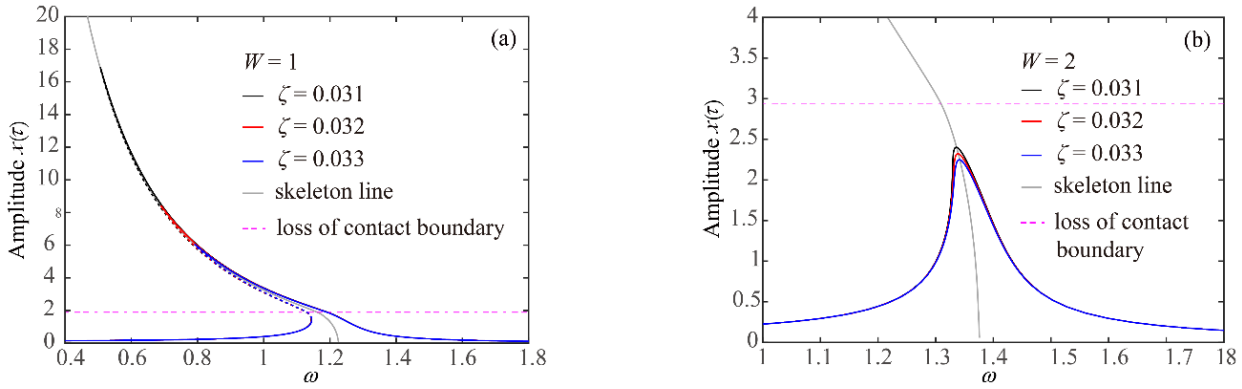

Figure 6. For α = 1.5, influence of ζ on the frequency-response peak-to-peak curves of one-sided contact system, (**a**) W = 1 and (**b**) W = 2.

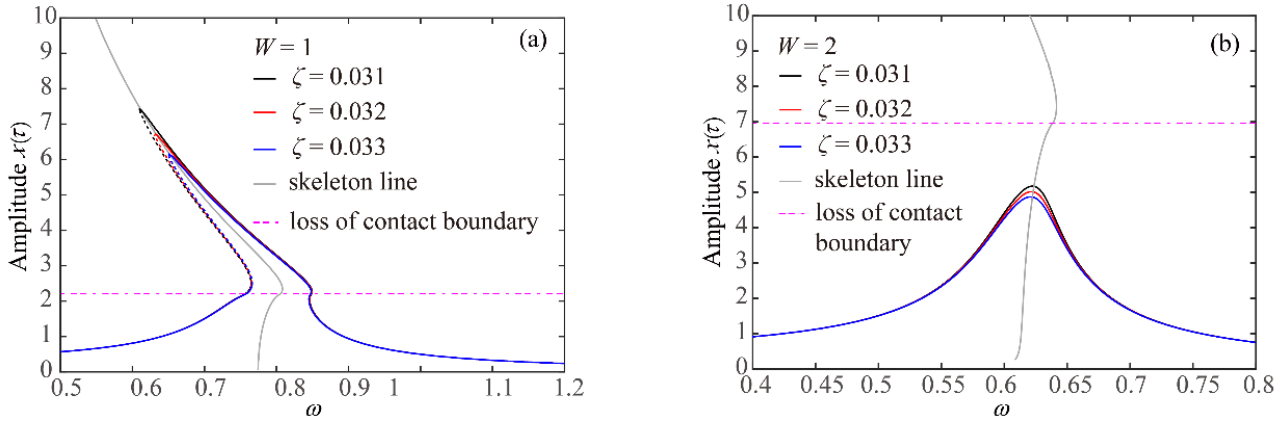

Figure 7. For α = 0.6, influence of ζ on the frequency-response peak-to-peak curves of one-sided contact system, (**a**) W = 1 and (**b**) W = 2.

4.3. Excitation Characteristics of One-Sided Contact System (ζ = 0.032, α = 1, W = 1)

Next, the excitation characteristics of the one-sided contact system will be considered in detail. As shown in Figure 8a, for ω = 1, with the increase in the excitation amplitude A, the stable response of period-1 solution branch undergoes period-doubling bifurcation at A_1, and the coming period-2 solution branch undergoes hysteresis and jumping at the cyclic folding bifurcation points A_2 and A_3, which agrees well with the numerical bifurcation diagrams shown in Figure 8b. The period-doubling bifurcation leads coexistence of the stable period-1 solution and period-2 solution in the system. For example, the period-1 solution P_1 and period-2 solution P_2 coexist when A = 1. On the other hand, for ω = 1 and A = 1, the corresponding period-1 solution P_1 and period-2 solution P_2 are located on the primary resonance and 1/2-order sub-harmonic resonance (see Figure 9a), respectively. It is indicated that the intrinsic triggering mechanism of period-doubling bifurcation at A_1 is the softening dynamic stiffness characteristics of the one-sided contact system, where the loss of contact nonlinearity leads to the softening 1/2-order sub-harmonic resonance and the corresponding period-2 motions excited. In addition, the system also has higher-order stable solutions such as period-3, period-4, and period-5 solution branches coexisting (see Figure 9b), and they are excited by softening 1/3-order, 1/4-order, and 1/5-order sub-harmonic resonances, respectively. It is clear that the coexisting solution characteristics of a one-sided contact system are complex due to the loss of contact nonlinearity. Besides, as shown in Figure 9a, unlike primary resonance, the 1/2-order subharmonic and 2-order super-harmonic resonances of the system can only be excited in the case of losing contact, because the system belongs to a linear continuous system (α = 1) below the loss of contact boundary.

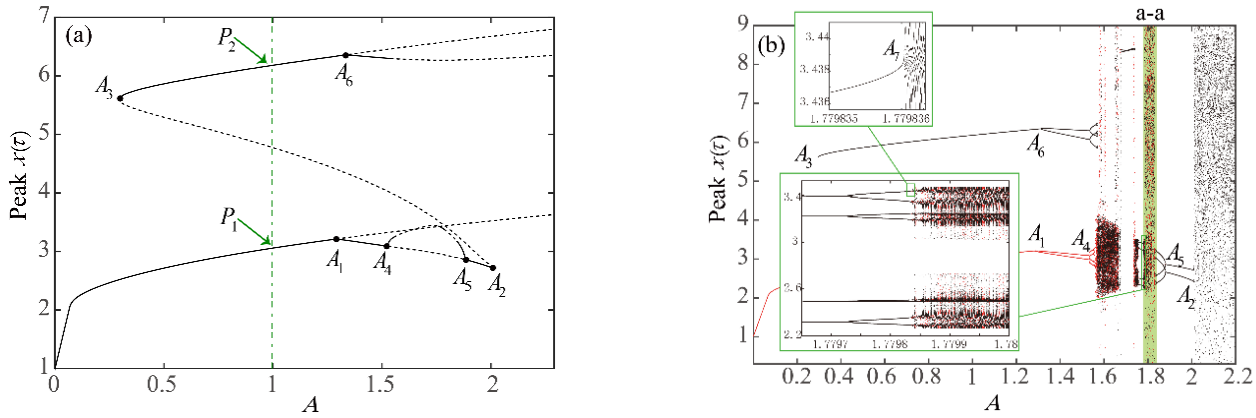

Figure 8. One-sided contact system for $\omega = 1$, (**a**) the periodic solution branch as the excitation amplitude A varies, and (**b**) numerical bifurcation diagrams of $x(\tau)$ when A sweeps up (black dots) and down (red dots).

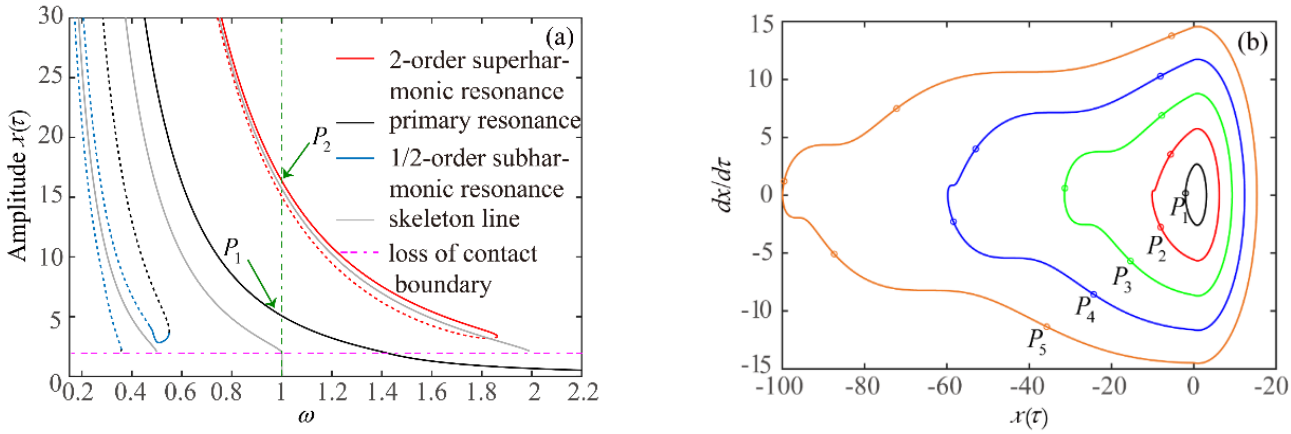

Figure 9. One-sided contact system for $A = 1$, (**a**) the frequency-response peak-to-peak curves, and (**b**) phase portraits their Poincare mapping dots of co-existing period-n solutions (i.e., P_n) when $\omega = 1$.

Moreover, as shown in Figure 8, the period-doubling bifurcations at points A_4 and A_6 lead to the period-4 solution branches excited from the stable period-2 branch, and then period-8 response also emerges through period-doubling of the period-4 solution branch. The leading Floquet multiplier of the coming period-8 solution branch passes out of the unit circle from the +1 axis at A_7 point of $A = 1.77983603$ as A changes (see Table 1), where the typical reverse tangent bifurcation [26,29] is clear (see Figure 8b), and then the motion of type-I intermittency chaos is induced (see Figure 10a). As the excitation amplitude A increases, the loses contact characteristics of the system become stronger, and the typical crisis-induced [30] intermittency chaos (see Figure 10b) emerges in the interval a-a of Figure 8b. At this time, the type-I intermittency chaos attractor merges with another periodic orbit, and Figure 11 shows the process of the above involution.

Table 1. Period-8 motion Floquet multipliers λ_m around the turning point A_8.

A	1.7798	1.77982	1.779835	1.77983603
λ_m	0.9920 0.1857	0.9927 0.1854	0.9991 0.1839	1.0020 0.1833

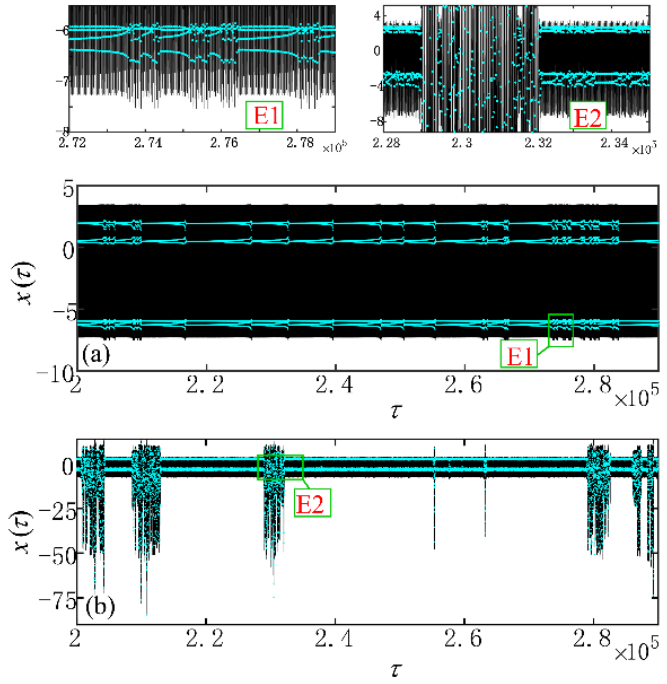

Figure 10. Time series $x(\tau)$ and their enlargements of one-sided contact system for $\omega = 1$, (**a**) $A = 1.78$, and (**b**) $A = 1.785$, where the cyan dots denote the period-1 mapping points of $x(\tau)$ at intervals of excitation period 2π.

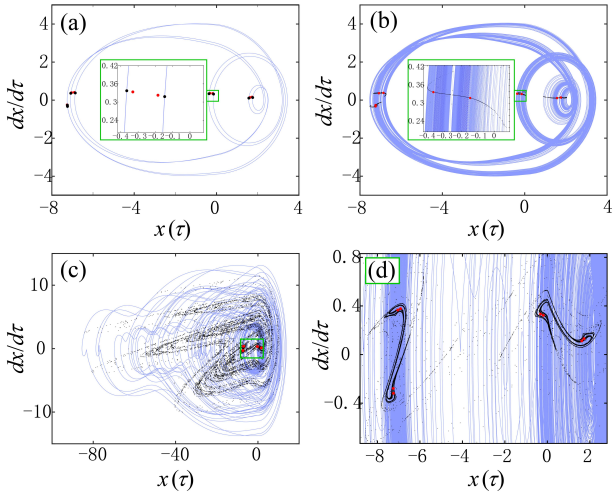

Figure 11. Phase portraits and their Poincare mappings of one-sided contact system for $\omega = 1$, (**a**) $A = 1.7798$, (**b**) $A = 1.78$, (**c**) $A = 1.785$, and (**d**) the enlargement of (**c**), where the red dots denote the Poincare mapping of unstable period-8 motion at A_7 point (see Figure 8).

5. Conclusions

Contact vibrations between relative moving components in contact systems, such as hinges, meshing gears, rolling bearings, and probe detection system, are often inevitable due to the external excitations or roughness and waviness between contact surfaces, where the power-form nonlinear load-deformation relationship $F_C(x) = K_C \cdot x^{\alpha}$ is commonly satisfied in the contact interfaces. With the aid of the HB–AFT method and Floquet theory, we have investigated the dynamic characteristics of the hardening/softening nonlinear stiffness and hysteretic resonances for the typical continuous and one-sided contact power-form spring systems. First, it is found that the externally normal load can lead to hardening-to-softening ($0 < \alpha < 1$) or softening-to-hardening ($\alpha > 1$ dynamic stiffness characteristics to the continuous power-form system, unlike the purely softening ($0 < \alpha < 1$) or hardening ($\alpha > 1$)

dynamic stiffness characteristics without an externally normal load. Second, it is shown that the one-sided contact power-form spring model can exhibit remarkable softening spring characteristics, and the resonant response amplitude is dramatically affected by the damping coefficient in the case of loss of contact. Third, the location of the primary resonance moves to a higher frequency ($\alpha > 1$) or lower frequency ($0 < \alpha < 1$) in either a continuous or one-sided system. Finally, it is indicated that multi-order super/sub-harmonic softening resonances and abundant bifurcation behaviors can also be excited beyond the loss of contact boundary, which can lead to multiple periodic solutions with different periods co-existing and can even excite type-I and crisis-induced intermittency chaos to the one-sided contact system. The results obtained in this paper could benefit to clarify the inherent correlations between dynamic stiffness characteristics and complex resonances in the vibrational contact systems.

Author Contributions: Conceptualization, Z.Z.; investigation, Z.Z., Q.W. and Y.Y.; methodology, Z.Z.; validation, Q.W., Z.Z. and Z.P.; supervision, Z.Z.; writing—original draft preparation, Q.W., Z.Z. and Y.Y. All authors have read and agreed to the published version of the manuscript.

Funding: This research was funded by China Postdoctoral Science Foundation (Grant No. 2019M661849), Jiangsu Planned Projects for Postdoctoral Research Funds (Grant No. 2018K164C), Fundamental Research Funds for the Central Universities (Grant No. 30920021155), Open-end Research Fund of State Key Laboratory of Mechanical Behavior and System Safety of Traffic Engineering Structures (Grant No. KF2020-30), and National Natural Science Foundation of China under (Grant No. 11802130).

Institutional Review Board Statement: Not applicable.

Informed Consent Statement: Not applicable.

Data Availability Statement: Not applicable.

Acknowledgments: Z.Z. gratefully acknowledges Thomas Sattel (Technische Universität Ilmenau), Yushu Chen and Qingjie Cao (Harbin Institute of Technology) for considerable help and valuable suggestions for the paper.

Conflicts of Interest: The authors declare no conflict of interest.

References

1. Holland, D.; Marder, M. Ideal brittle fracture of silicon studied with molecular dynamics. *Phys. Rev. Lett.* **1998**, *80*, 746–749. [CrossRef]
2. Valtonen, M.; Karttunen, H. *The Three-Body Problem*; Cambridge University Press: Cambridge, UK, 2006.
3. Ibrahim, R.A. *Vibro-Impact Dynamics*; Springer: Berlin/Heidelberg, Germany, 2009.
4. Russell, D.; Rossing, T. Testing the nonlinearity of piano hammers using residual shock spectra. *Acta Acust. United Acust.* **1998**, *84*, 967–975.
5. Manciu, M.; Sen, S.; Hurd, A.J. The propagation and backscattering of soliton-like pulses in a chain of quartz beads and related problems. (I). Propagation. *Phys. A* **2000**, *274*, 588–606. [CrossRef]
6. Xiao, H.F.; Sun, Y.Y. On the normal contact stiffness and contact resonance frequency of rough surface contact based on asperity micro-contact statistical models. *Eur. J. Mech. A-Solid* **2019**, *75*, 450–460. [CrossRef]
7. While, M.F. Rolling element bearing vibration transfer characteristics: Effect of stiffness. *ASME J. Appl. Mech.* **1979**, *46*, 677–684. [CrossRef]
8. Yu, X.; Sun, Y.Y.; Zhao, D.; Wu, S. A revised contact stiffness model of rough curved surfaces based on the length scale. *Tribol. Int.* **2021**, *164*, 107206. [CrossRef]
9. Hess, D.; Soom, A. Normal vibrations and friction under harmonic loads: Part 1: Hertzian contact. *ASME J. Tribol.* **1991**, *113*, 80–86. [CrossRef]
10. Harris, T.A. *Rolling Bearing Analysis*, 4th ed.; John Wiley & Sons: New York, NY, USA, 2001.
11. Ehrich, F.F. *Handbook of Rotordynamics*; McGraw-Hill: New York, NY, USA, 1992.
12. Zhang, Z.Y.; Sattel, T.; Aditya, S.T.; Rui, X.; Yang, S.; Yang, R.; Ying, Y.; Li, X. Suppression of complex hysteretic resonances in varying compliance vibration of a ball bearing. *Shock Vib.* **2020**. [CrossRef]
13. Oliva Uribe, D.; Schoukens, J.; Stroop, R. Improved tactile resonance sensor for Robotic assisted surgery. *Mech. Syst. Signal. Pr.* **2018**, *99*, 600–610. [CrossRef]
14. Aureli, M.; Tung, R. A plate-like sensor for the identification of sample viscoelastic properties using contact resonance Atomic Force Microscopy. *ASME Lett. Dyn. Sys. Control.* **2021**, *1*, 1–9.
15. Mickens, R.E. Analysis of non-linear oscillators having nonpolynomial elastic terms. *J. Sound Vib.* **2002**, *255*, 789–792. [CrossRef]
16. Hu, H.; Xiong, Z.G. Oscillations in an x(2m+2)/(2n+1) potential. *J. Sound Vib.* **2003**, *259*, 977–980. [CrossRef]
17. Cveticanin, L. Oscillator with fraction order restoring force. *J. Sound Vib.* **2009**, *320*, 1064–1077. [CrossRef]

18. Kovacic, I.; Rakaric, Z.; Cveticanin, L. A non-simultaneous variational approach for the oscillators with fractional-order power nonlinearities. *Appl. Math. Comput.* **2010**, *217*, 3944–3954. [CrossRef]
19. Kovacic, I. Forced vibrations of oscillators with a purely nonlinear power-form restoring force. *J. Sound Vib.* **2011**, *330*, 4313–4327. [CrossRef]
20. Rakaric, Z.; Kovacic, I. An elliptic averaging method for harmonically excited oscillators with a purely non-linear non-negative real-power restoring force. *Commun. Nonlinear Sci. Numer. Simul.* **2013**, *18*, 1888–1901. [CrossRef]
21. Huang, D.M.; Xu, W.; Liu, Y.J.; Liu, Y. Dynamical properties of a forced vibration isolation system with real-power nonlinearities in restoring and damping forces. *Nonlinear Dyn.* **2015**, *81*, 641–658. [CrossRef]
22. Carson, R.M.; Johnson, K.L. Surface corrugations spontaneously generated in a rolling contact disc machine. *Wear* **1971**, *17*, 59–72. [CrossRef]
23. Nayak, R. Contact vibrations. *J. Sound Vib.* **1972**, *22*, 297–322. [CrossRef]
24. Rigaud, E.; Perret-Liaudet, J. Experiments and numerical results on nonlinear vibrations of an impacting Hertzian contact. Part 1: Harmonic excitation. *J. Sound Vib.* **2003**, *265*, 289–307. [CrossRef]
25. Ma, Q.L.; Kahraman, A.; Perret-Liaudet, J.; Rigaud, E. An investigation of steady-state dynamic response of a sphere-plane contact interface with contact loss. *ASME J. Appl. Mech.* **2007**, *74*, 249–255. [CrossRef]
26. Zhang, Z.Y.; Rui, X.T.; Yang, R.; Chen, Y. Control of period-doubling and chaos in varying compliance resonances for a ball bearing. *ASME J. Appl. Mech.* **2020**, *87*, 021005. [CrossRef]
27. Zhang, Z.Y.; Sattel, T.; Zhu, Y.J.; Dong, Y.; Rui, X. Mechanism and characteristics of global varying compliance parametric resonances in a ball bearing. *Appl. Sci.* **2020**, *10*, 7849. [CrossRef]
28. Jackson, S.; Gutschmidt, S.; Roeser, D.; Sattel, T. Development of a mathematical model and analytical solution of a coupled two-beam array with nonlinear tip forces for application to AFM. *Nonlinear Dyn.* **2017**, *87*, 775–787. [CrossRef]
29. Manneville, P.; Pomeau, Y. Intermittency and the Lorenz model. *Phys. Lett. A* **1979**, *75*, 1–2. [CrossRef]
30. Yue, Y.; Miao, P.C.; Xie, J.H.; Celso, G. Symmetry restoring bifurcations and quasiperiodic chaos induced by a new intermittency in a vibro-impact system. *Chaos* **2016**, *26*, 113121. [CrossRef]